ACADEMIC PRESS

Available online at www.sciencedirect.com

SCIENCE DIRECT®

DEVELOPMENTAL BIOLOGY

Developmental Biology 253 (2003) 230–246

www.elsevier.com/locate/ydbio

Requirement for tumor suppressor Apc in the morphogenesis of anterior and ventral mouse embryo

Tomo-o Ishikawa,[a] Yoshitaka Tamai,[b] Qin Li,[a] Masanobu Oshima,[a] and Makoto M. Taketo[a,c,*]

[a] *Department of Pharmacology, Graduate School of Medicine, Kyoto University, Kyoto, 606-8501, Japan*

[b] *Banyu Tsukuba Research Institute (Merck), Tsukuba, 300-2611, Japan*

[c] *Graduate School of Pharmaceutical Sciences, University of Tokyo, Tokyo, 113-0033, Japan*

Received for publication 14 August 2002, revised 8 October 2002, accepted 8 October 2002

Abstract

Tumor suppressor Apc (adenomatous polyposis coli) is implicated in the Wnt signaling pathway that is involved in the early embryonic development and tumorigenesis in vertebrates. While the heterozygous null mutant mice develop intestinal polyps, the homozygous embryos die before gastrulation. To investigate the role of Apc in later embryonic development, we constructed a novel hypomorphic *Apc* allele whose expression was attenuated by ~80%. In the hypomorphic *Apc* homozygous ES cells, reduction in Apc expression caused β-catenin accumulation and Wnt signaling activation. The homozygous mutant mouse embryos survived 3 days longer than the null mutant embryos. Interestingly, they showed anterior truncation, partial axis duplication, and defective ventral morphogenesis. To determine the tissues where *Apc* functions for anterior and ventral morphogenesis, we constructed chimeric embryos whose epiblast was derived predominantly from the *Apc* hypomorphic homozygous cells but the visceral endoderm was from the wild type. Although these chimeric embryos still showed some anterior defects, their ventral morphogenesis was rescued. In addition, marker studies indicated that the axial mesendoderm was also defective in the homozygous embryos. Our results provide genetic evidence that expression of Apc at the normal level is essential for both anterior and ventral development, in the epiblast derivatives and visceral endoderm.

Keywords: AME; AVE; Foregut; Heart; Morphogenesis; Wnt signaling

Introduction

The Wnts consist of a family of secretory polypeptides related to *Drosophila wingless* (Nusse, 1997; Wodarz and Nusse, 1998). When they bind to the frizzled family receptors, the signal is transduced through cytoplasmic proteins and inhibits glycogen synthase kinase 3β (GSK-3β). The GSK-3β substrates include β-catenin as well as the negative regulator Apc. Mutations in the adenomatous polyposis coli (*APC*) gene (Groden et al., 1991; Kinzler et al., 1991) cause an accumulation of unphosphorylated β-catenin. Unlike phosphorylated β-catenin that is degraded rapidly by ubiquitination, unphosphorylated β-catenin is stable and accumulates in the cytoplasm, moves into the nucleus, and activates transcription of a new set of genes by binding to the Tcf/Lef complex (Polakis, 1999). The biological consequences of excessive Wnt signaling in vertebrates are formation of a secondary axis in the embryo (Nusse, 1997; Wodarz and Nusse, 1998) and tumorigenesis in adults (Polakis, 2000; Bienz and Clevers, 2000). While heterozygous *Apc* mutant mice develop intestinal polyps, like in the human familial adenomatous polyposis patients, the homozygous embryos die before gastrulation (Moser et al., 1995; Oshima et al., 1995).

Although the molecular control of axis development in mammalian embryos has not been elucidated thoroughly, some insights have been obtained through the studies on

* Corresponding author. Department of Pharmacology, Graduate School of Medicine, Kyoto University, Yoshida-Konoé-cho, Sakyo-ku, Kyoto, 606-8501, Japan. Fax: +81-75-753-4402.

E-mail address: taketo@mfour.med.kyoto-u.ac.jp (M.M. Taketo).

0012-1606/03/$ – see front matter © 2003 Elsevier Science (USA). All rights reserved.
PII: S0012-1606(02)00020-9

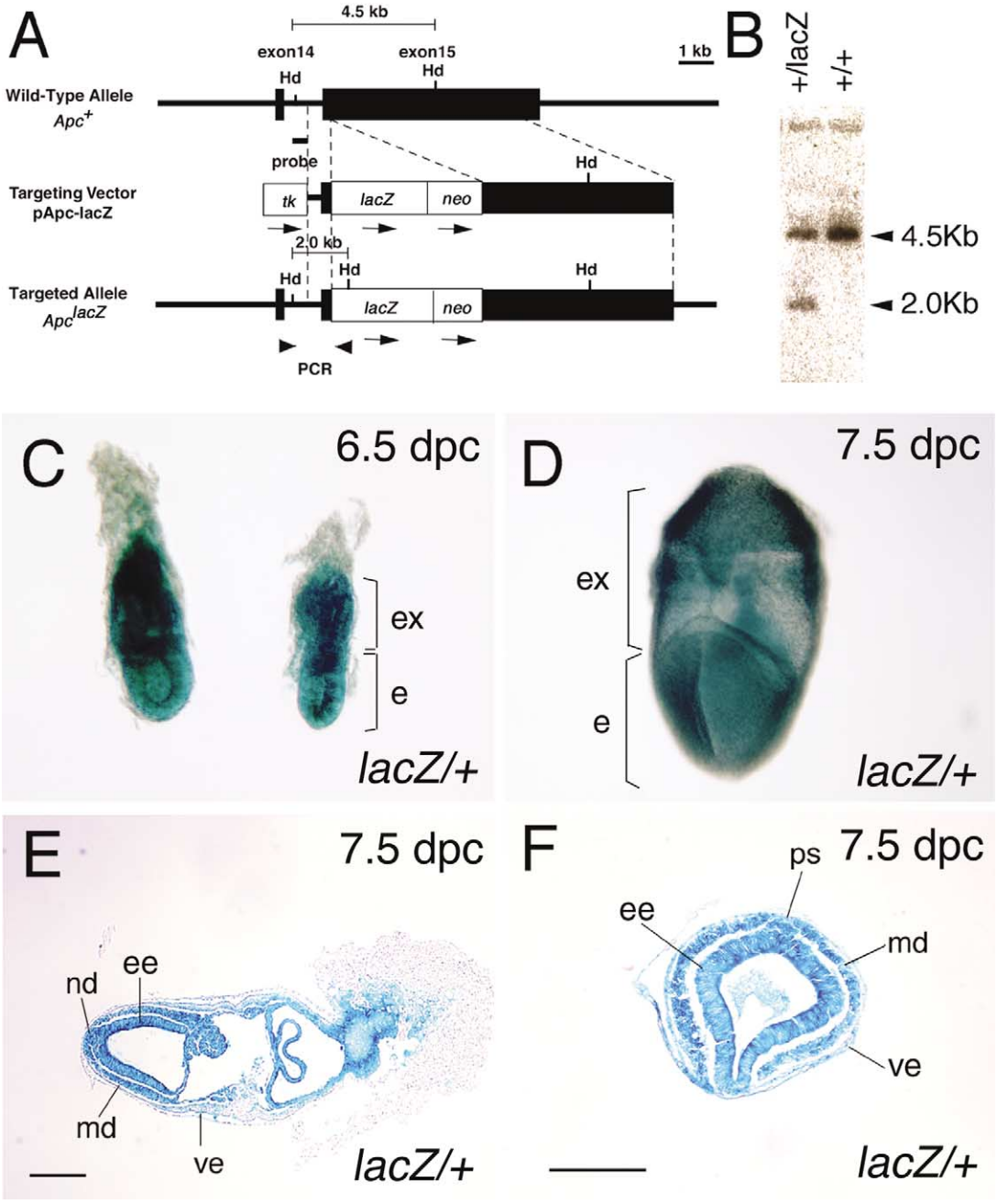

Fig. 1. Expression of *Apc* in the mouse embryos at 6.5–7.5 dpc monitored by the lacZ activity. (A) Targeting strategy for construction of Apc^{lacZ} mice. (Top) Wild-type allele Apc^{+}. (Middle) Targeting vector pApc-lacZ. (Bottom) Targeted allele Apc^{lacZ}. Exons are shown as filled boxes, whereas intronic sequences are solid lines. The *lacZ*, PGK-*neo (neo)* and PGK-*tk (tk)* cassettes are shown as open boxes with their transcriptional orientations (arrows). The PCR primers and Southern hybridization probe are shown as a pair of arrowheads and a solid line, respectively. The *Hin*dIII fragments hybridizable to the probe are also shown (4.5 and 2.0 kb for the wild-type and targeted alleles, respectively). Hd, *Hin*dIII sites. (B) Verification of the homologous recombination in an ES cell clone by Southern hybridization. Extracted DNA samples were digested with *Hin*dIII and hybridized with the probe shown in (A). (C) Expression of the Apc^{lacZ} gene in heterozygous embryos (*lacZ*/+) at 6.5 dpc. Note the ubiquitous staining in the whole embryo. (D) Expression of the Apc^{lacZ} gene in a heterozygous embryo at 7.5 dpc. Note that the β-galactosidase activity is found in both embryonic (e) and extraembryonic (ex) regions ubiquitously. (E) A sagittal section of a 7.5-dpc embryo. (F) A transverse section through the embryo proper at 7.5 dpc. Note that lacZ is expressed in all three germ layers. ee, embryonic ectoderm; md, mesoderm; nd, node; ps, primitive streak; and ve, visceral endoderm. Scale bars, 100 μm.

such mouse mutants as *fused* (*Axin*, formerly called, *Fu*) (Gluecksohn-Shoenheimer, 1949; Jacobs-Cohen et al., 1984; Perry et al., 1995). In addition to neuroectodermal and cardiac abnormalities, early postimplantation embryos homozygous for these mutant alleles show a remarkable duplication of the embryonic axis. Through the analysis of the transgenic insertion in Fu^{Tg1}, a cDNA was cloned which encoded *Axin* (Zeng et al., 1997). Subsequent analyses

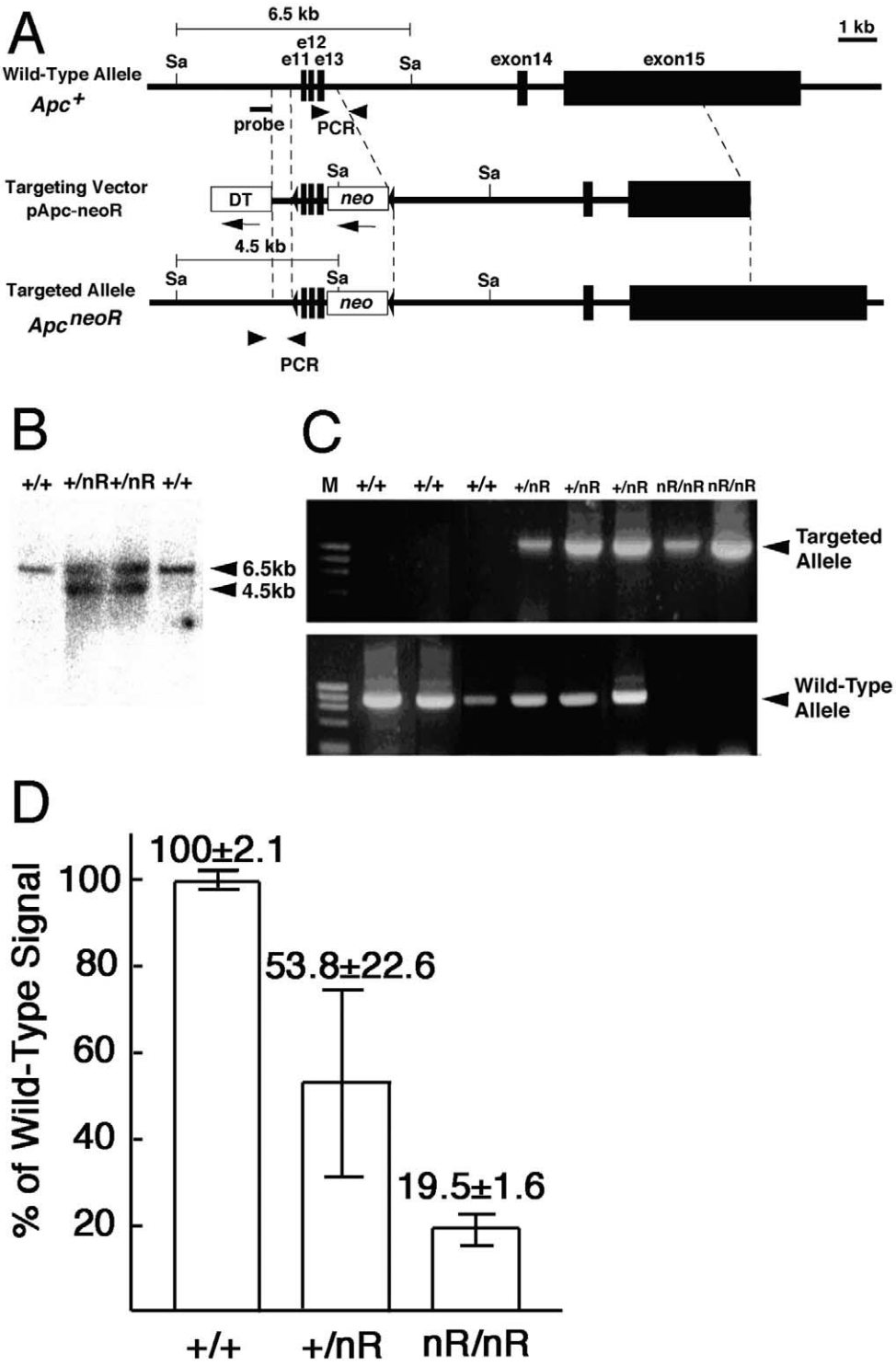

Fig. 2. Construction of the hypomorphic *Apc* mutant mice. (A) Targeting strategy. (Top) Wild-type allele Apc^{+}. (Middle) Targeting vector pApc-neoR. (Bottom), Targeted allele Apc^{neoR}. Exons are shown as filled boxes, whereas intronic sequences are solid lines. The PGK-*neo (neo)* and PGK-DT (DT) cassettes are shown as open boxes with their transcriptional orientations (arrows). Triangles sandwiching exons 11–13 and the PGK-*neo* cassette indicate *loxP* sequences. The PCR primers and Southern hybridization probe are shown as pairs of arrowheads and a solid line, respectively. *Sac*1 fragments hybridizable to the probe are also shown (6.5 kb and 4.5 kb for the wild-type and targeted alleles, respectively). Sa, *Sac*I sites. (B) Confirmation of the homologous recombination in ES cell clones by Southern hybridization. Extracted DNA samples were digested with *Sac*I and hybridized with the probe shown in (A). (C) PCR genotyping of the 8.5-dpc embryonic DNA from a heterozygous intercross. (Top) Primers for the targeted allele. (Bottom) Primers for the wild-type allele. Genotypes are shown on top of the lanes: +, wild-type allele; and nR, *neoR* allele. Lane M was loaded with size markers. (D) Determination of the *Apc* mRNA expression in Apc^{neoR} mouse embryos by the TaqMan method of RT-PCR. Relative amounts of *Apc* mRNA for the Apc^{neoR} heterozygote and homozygote to that of the wild type are shown with standard deviations. Bars +/+, +/*nR*, and *nR/nR* indicate the genotypes for the wild-type, heterozygous, and homozygous Apc^{neoR} mutant embryos, respectively.

Table 1
Genotypes of the Apc^{neoR} intercross offspring

Age (dpc)	Genotypes[a]		
	(+/+)	(+/*neoR*)	(*neoR*/*neoR*)
7.5	30[b]		8[c]
8.5	21	23	17[c]
9.5	13	21	7[c]
10.5	3	2	2[c]
12.5	5	11	0
Live born	56	72	0

[a] (+/+), wild type; (+/*neoR*), heterozygous Apc^{neoR}; and (*neoR*/*neoR*), homozygous Apc^{neoR}.
[b] The wild type and heterozygote numbers combined.
[c] With abnormal morphology under a dissection microscope.

showed that axin is an inhibitor of the Wnt signaling pathway and binds to β-catenin, GSK3β, and Apc. Because the axis determination in mammalian embryos takes place in a much later stage than in amphibian embryos (Beddington and Robertson, 1998, 1999), the role of Apc in the axis determination could be masked by the death of the homozygous embryo prior to the axis determination when studied in the null mutant *Apc* mouse. To overcome this problem, we have constructed by homologous recombination in ES cells a novel mutant *Apc* allele whose expression is attenuated, but not totally inactivated. Here, we present the phenotypes of the mouse embryos with the hypomorphic *Apc* allele and those with additional null *Apc* allele.

Materials and methods

Targeting vector construction

Mouse genomic DNA fragments of *Apc* were isolated by screening a 129/Sv mouse genomic library in a bacteriophage λ vector (Stratagene) as described previously (Oshima et al., 1995). To construct pApc-lacZ, the IRES-lacZ cassette and the PGK-*neo*-bpA cassette were inserted into the *Nco*I site at the beginning of exon 15 (base no. 2150). The HSV thymidine kinase gene driven by the PGK promoter was inserted at an upstream *Sac*I site. To construct pApc-neoR, a 1.0-kb *Xba*I–*Hin*dIII fragment containing exons 11–13, and the PGK-*neo*-bpA cassette were cloned into a *loxP*-containing vector pBS246 (Gibco-BRL). To the resulting plasmid, the following fragments were inserted further: a 10-kb *Hin*dIII fragment (containing exon 14 and a part of exon 15), a 1.0-kb *Sac*I–*Xba*I fragment (containing intron 10) of *Apc*, and the PGK-DT cassette (Oshima et al., 1995).

ES cell culture, chimera construction, and germline transmission

ES cell line RW4 (Genome Systems) was cultured on primary mouse embryo fibroblasts (MEFs), and 2×10^7 cells were electroporated as described (Oshima et al., 1995). Homologous recombinant candidates were screened by PCR. To genotype Apc^{lacZ} ES clones and mice, the following primer set was used; P91 in intron 14 (5′-GGC TCA GCG TTT TCC TAA TGA TGT C-3′) and P92 in IRES (5′-TCA CGA CAT TCA ACA GAC CTT G-3′) to amplify a 1.2-kb fragment. To genotype Apc^{neoR} ES clones and mice, the following primer sets were used; for the targeted allele, P83 in the *loxP* flanking sequence (5′-GGA CGT AAA CTC CTC TTC AGA CCT-3′) and P86 in intron 10 (5′-CAG GGT TGT TTC TCA GAC CCT TTC C-3′), to amplify a 1.3-kb fragment; and for the wild-type allele, P72 in exon 11 (5′-CTT TGA CAA ACT TGA CCT TTG GAG ATG TTG-3′) and P94 in intron 14 (5′-AAA GCC ATA CTT TAA CAC AAG CCA C-3′), to amplify an 0.9-kb fragment. Homologous recombination in ES cells was verified by Southern hybridization using the probes shown in Fig. 1A or 2A, as described previously (Oshima et al., 1995). Chimeras were generated by injecting the ES cells into C57BL/6N blastocysts.

Histochemical localization of the β-galactosidase activity

For the timing of embryos, the day of the vaginal plug was considered as 0.5 dpc. When removed from the decidua, embryos were staged according to Kaufman (1992). To detect the β-galactosidase activity, the samples were incubated at 30°C overnight in a staining solution (5 mM potassium ferricyanide, 5 mM potassium ferrocyanide, 1 mg/ml X-gal in PBS).

Generation of the homozygous Apc^{neoR} ES cells

One heterozygous Apc^{neoR} ES clone, which transmitted the targeted allele through the germ line, was cultured in a medium containing 3.75 mg/ml geneticin (Mortensen et al., 1992). To screen for homozygous recombinants, DNA from the surviving clones was analyzed by PCR, using primers P72 and P94 and verified further by Southern hybridization with the probes shown in Fig. 2A.

Generation and analysis of chimeras

Chimeric embryos were obtained by injecting the two independent Apc^{neoR} ES cell clones into *Gt(Rosa)26Sor*/+ blastocysts. Injected blastocysts were transferred into pseudopregnant females, and embryos were recovered at 8.5–9.5 dpc. Both homozygous Apc^{neoR} ES cell clones gave rise to morphologically similar chimeras. The degree of chimerism was estimated by whole-mount staining of the embryos with X-gal.

Expression of Apc mRNA

To quantify the transcripts from the *Apc* hypomorphic allele, we used the TaqMan procedure with an ABI PRISM

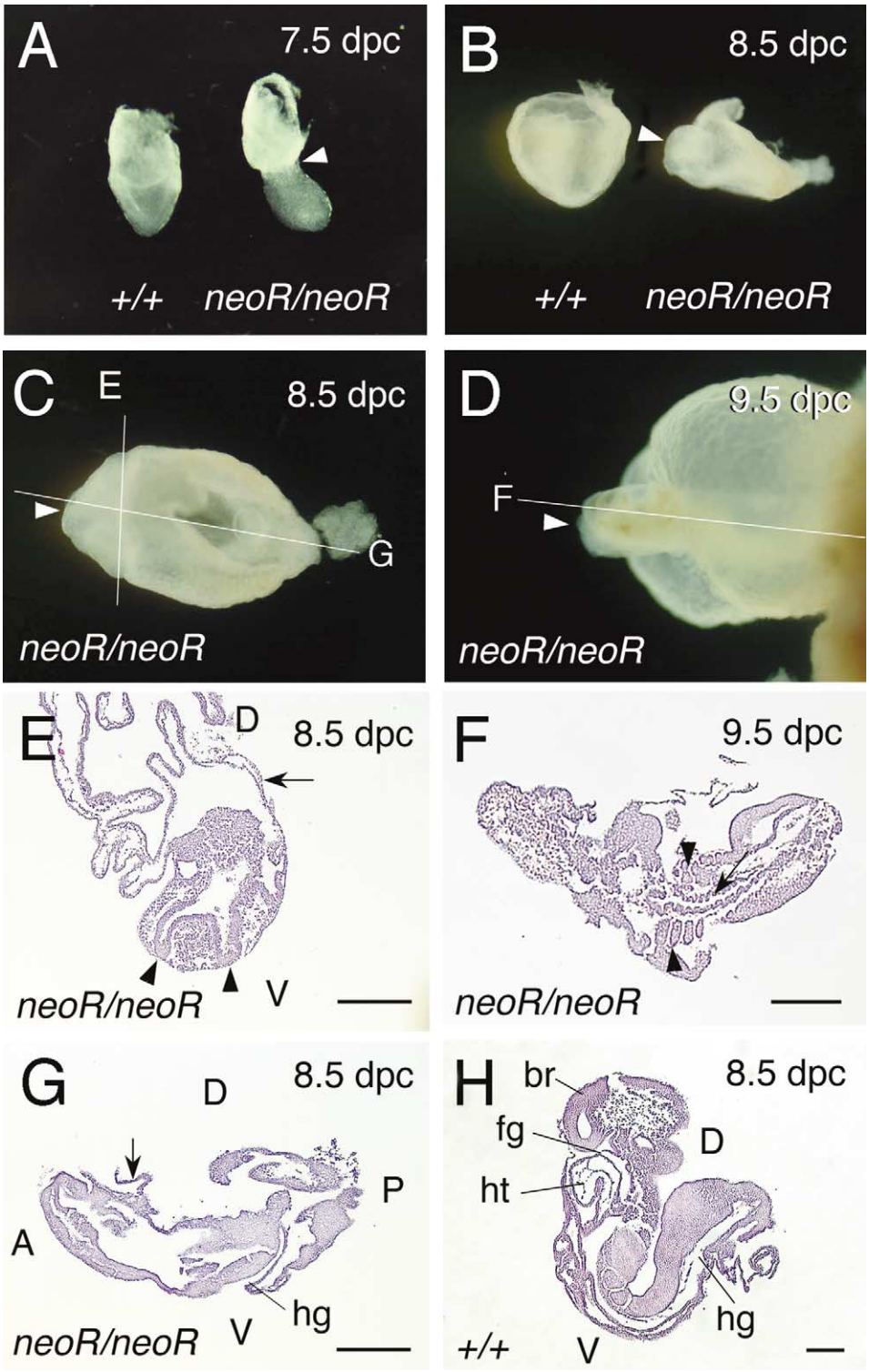

Fig. 3. Morphology of the homozygous *Apc*^{neoR} *neoR/neoR* embryos. (A) Embryos at 7.5 dpc. Note the constricted appearance between the embryonic and extraembryonic portions in the (*neoR/neoR*) embryo (arrowhead). (B) Embryos at 8.5 dpc. Note that the head is outside the yolk sac in the *neoR/neoR* embryo (arrowhead; see C). (C) The 8.5-dpc *neoR/neoR* embryo in (B) at a higher magnification. Lines E and G indicate the sectioning planes shown in photographs E and G, respectively. (D) The 9.5-dpc *neoR/neoR* embryo. Note the protruded head from the yolk sac (arrowhead). Line F indicates the sectioning plane in photograph F. (E) A transverse section (through line E in photograph C) of the 8.5-dpc embryo. Note the duplicated neural tube at the anterior end (arrowheads) protruding from the yolk sac (arrow). (F) A frontal section (through line F in photograph D) of the homozygous embryo at 9.5 dpc. Note that the neural tube is deformed (arrow), but some somites are formed (arrowheads). (G) A sagittal section (through line G in photograph C) of the 8.5-dpc *neoR/neoR* embryo. Note that the brain is poorly formed with the head portion of the embryo outside the yolk sac (arrow). The heart and foregut are not visible, although its precursors were formed (see Fig. 6B, below). (H) A sagittal section of an 8.5-dpc wild-type embryo shown as a control. Where appropriate, the embryonic polarities are shown by: A, anterior; P, posterior; D, dorsal; and V, ventral; whereas the organs are abbreviated as: br, brain; ht, heart; fg, foregut; and hg, hindgut. (A–D) Dissection micrographs; (E–H) Histological sections (H&E). Scale bars, 500 μm.

7700 thermal cycler and detector according to the manufacturer's protocol. The pooled total RNA was isolated from the 9.5 days post coitum (dpc) embryos with Sepagene (Nacarai Tesque) and purified by RNeasy Mini Kits (QIAGEN). The total RNA was then reverse-transcribed by using the TaqMan RT Reagent Kit (Applied Biosystems) with random primers. The resulting cDNA was amplified by using TaqMan PCR Core Reagents (Applied Biosystems) with an *Apc*-specific primer set in exon 15; Apc1777 (5′-CTG TCT GCA CAC TGC ACT GAG A-3′) and Apc1878 (5′-AGT ATT TGC TGG CTC CGG TAA GT-3′). The products were detected with TaqMan fluorescent probe Apc1827 (5′-Fam-TCC ATC CAC AGC ACA GAT GTC AGC CT-Tamra-3′) purchased from Applied Biosystems. Triplicate samples of the total RNA from each genotype were analyzed, and a control lacking reverse transcriptase was run to rule out contaminating genomic DNA. The amounts of *Apc* mRNA from the heterozygous and homozygous Apc^{neoR} embryos were compared with those from the wild-type embryos after calibration to the amounts of the glycerol-3-phosphate dehydrogenase gene (G3PDH) mRNA internal control (TaqMan Rodent G3PDH Control Reagents, VIC Probe; Applied Biosystems).

For semiquantitative RT-PCR of the *Apc* mRNA, RNA was extracted by using Isogen (Nippon Gene), reverse-transcribed with RNA-PCR kits (Takara), and amplified by using the following primers: P69 for *Apc* exon 13 (5′-TGG AAG TGT GAA AGC ATT GAT GGA ATG TGC-3′), and P68 in exon 15 (5′- CCA CAT GCA TTA CTG ACT ATT GTC AAG-3′). The G3PDH primers were purchased from Clontech. To analyze possibly aberrantly spliced transcripts involving the *neo* gene, various segments between *neo* and *Apc* exons 11–14 were amplified by using five sets of primers: P71 in exon 12 (5′-CTA TGA AAG GCT GCA TGA GAG CAC TTG TGG-3′); P72 in exon 11 above; P23 in exon 3 (5′-GGG GTC ATT CCC AAG AAG AAC ATT TGT AAA T-3′); P24 in exon 4 (5′-AAG TTG AGC ATA ATA CCA GTC CTT TTC CTT C-3′); IMR-013 in *neo* (5′-CTT GGG TGG AGA GGC TAT T-3′); and neoU in *neo* (5′-ATC GCC TTC TAT CGC CTT CTT G-3′). The mRNA levels in the Apc^{neoR} embryos were estimated by RT-PCR at the amplification cycle number that was chosen for each genotype, where a linear relationship was obtained for both the *Apc* and *G3PDH* mRNAs.

Western immunoblotting

ES cells were lysed in buffer A (10 mM Hepes, pH 7.8, 10 mM KCl, 0.1 mM EDTA, 0.1% NP-40) on ice for 30 min. For the detection of β-catenin protein, nuclear/membrane fractions were separated by centrifugation at 2000*g* for 1 min at 4°C. An aliquot (10 μg protein) of each fraction was separated by 10% SDS–PAGE, blotted, and detected with monoclonal antibodies against nuclear β-catenin (8E4, 1:200; Alexis Biochemicals) and β-actin (AC-74, 1:2000; Sigma). For detection of Apc protein, 100 μg of protein from the total cell lysate was separated by 4% SDS–PAGE. An antibody to Apc (AFPN, 1:2000) was kindly provided by Dr. R. Fodde. The signals were visualized with ECL Detection System (Amersham Pharmacia Biotech).

β-Catenin/TCF reporter analysis

Approximately 10^6 undifferentiated ES cells were plated on six-well tissue culture plates coated with MEF feeder cell layer 24 h before transfection. Cells in each well were transfected with 500 ng TOPFLASH or FOPFLASH vector (Upstate Biology), and 500 ng CMV-LacZ vector using Lipofectamine 2000 (Invitrogen) according to the manufacturer's protocol. Luciferase activities were determined after 24 h with Luciferase Assay System (Promega) in a luminometer (Lumat LB9507; Perkin Elmer) and normalized for the transfection efficiency based on the β-galactosidase activity determined with β-Galactosidase Enzyme Assay System (Promega).

In situ hybridization analyses

Whole-mount samples were hybridized with RNA probes labeled with digoxigenin-11-UTP (Roche Diagnostics) as described (Saga et al., 1996). The *Six3* probe was prepared from cDNA template amplified by PCR using the following primers: Primer F, 5′-GGA AGA GTT GTC CAT GTT CCT GTT G-3′, and Primer R, 5′-ATT CCG AGT CGC TGG AGG TTA CCG A-3′. The probes for *Otx2* and *Egr2* (*Krox-20*) were obtained from S. Aizawa and D. Wilkinson, respectively. The probes for *Wnt1* and *Shh* were obtained from A. McMahon. The *Hoxb*1 probe was prepared from cDNA templates amplified by PCR using the following primers: Primer F, AGA TGC CTC TGA CCA GTC CGC GTG CAC CTC, and Primer R, TTG GCT GGA TTA AGA TTA AGG GTT GGT GGC. The *T (Brachury)* probe was derived from an EST clone (Accession No. AA068174). The probes for *Foxa1 (Hnf3a)* and *Foxa2 (Hnf3b)* were obtained from H. Sasaki, whereas the probe for *Noda*l was from Y. Saga. The MHC (*Myhca*), cardiac troponin C, and *Gata4* probes were prepared from cDNA templates amplified by PCR using the primers described in Kuo et al. (1997).

Histology

For paraffin sectioning, samples were fixed in 4% paraformaldehyde and embedded according to the standard procedure.

Results

Ubiquitous expression of Apc mRNA at the gastrulation stage

To monitor the *Apc* expression in early embryonic development, we constructed knockout mice with a bacterial β-galactosidase (*lacZ*) reporter gene using a standard gene

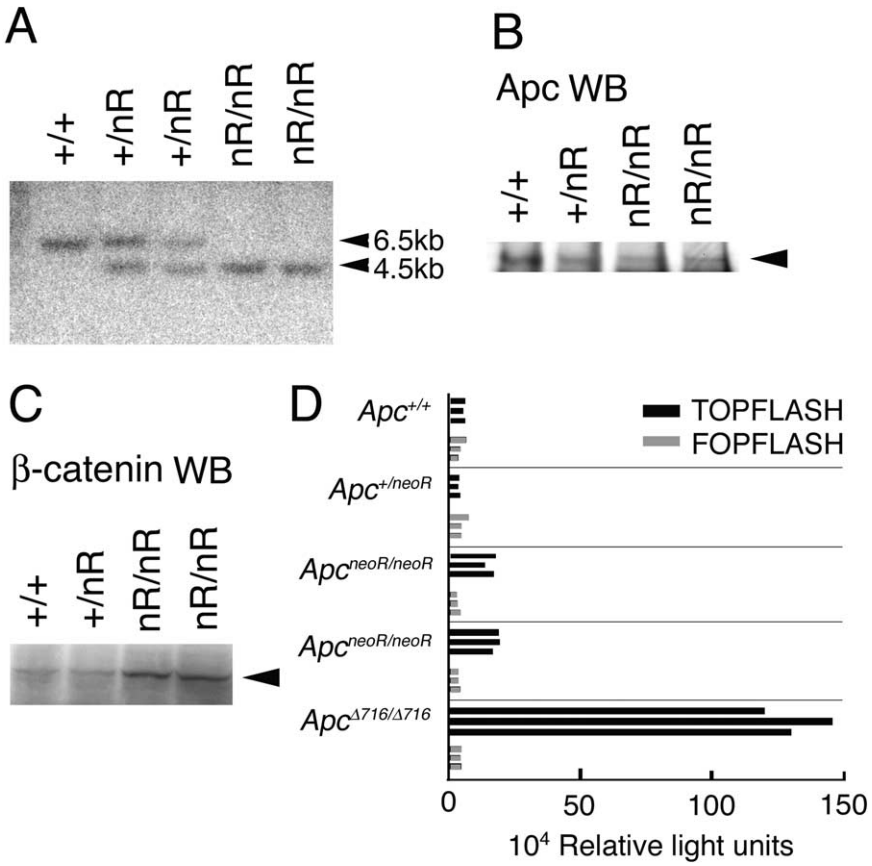

Fig. 4. Isolation and analysis of the homozygous Apc^{neoR} ES cells. Genotypes are: +/+, wild type; +/*nR*, heterozygous Apc^{neoR}; and *nR/nR*, homozygous Apc^{neoR}. (A) Genotyping by Southern hybridization of the ES cell clones isolated with 3.75 mg/ml geneticin. Extracted DNA samples were digested with *Sac*I and hybridized with the probe shown in Fig. 2A. (B) Western blot (WB) analysis of Apc protein in the wild-type, heterozygous, and homozygous Apc^{neoR} ES cells. (C) Western blot (WB) analysis of β-catenin protein in the Apc^{neoR} ES cells. The nuclear fractions were analyzed by using antibody against β-catenin for the parental wild-type, heterozygous, and homozygous Apc^{neoR} ES cells. (D) Transcriptional reporter assay for β-catenin/TCF in the wild-type, heterozygous Apc^{neoR}, homozygous Apc^{neoR}, and homozygous $Apc^{\Delta 716}$ ES cells. Two independent homozygous Apc^{neoR} clones were assayed. Undifferentiated ES cells were transfected with either TOPFLASH or FOPFLASH luciferase reporter construct with the internal control CMV-lacZ. Luciferase activity of the TOPFLASH or FOPFLASH reporter calibrated to the lacZ is shown for each ES cell line in triplicate transfections.

targeting strategy (Fig. 1A and B). The reporter gene was inserted at codon 716. The phenotypes of these mice were the same as those of the $Apc^{\Delta 716}$ mice (Oshima et al., 1995). Namely, the homozygous embryos were lethal, whereas the heterozygous mice developed intestinal adenomas. Using the heterozygous embryos, we determined the lacZ reporter activity by whole-mount in situ staining. The lacZ activity was expressed ubiquitously in the postimplantation embryo (Fig. 1C–F). At 6.5 dpc, a strong expression was observed throughout the embryonic and extraembryonic tissues (Fig. 1C), which persisted beyond 7.0 dpc (Fig. 1D). Embryonic sections showed lacZ expression in the epiblast, mesoderm, visceral endoderm, primitive streak, and the node (Fig. 1E and F). These results show that the *Apc* gene is expressed ubiquitously at the gastrulation stage.

Construction of hypomorphic allele Apc^{neoR}

In a series of attempts to investigate the function of Apc in developmental processes, we constructed a targeting vector for a new allele, Apc^{neoR} (where R stands for the reverse orientation; Fig. 2A). The targeted ES cells (Fig. 2B) were injected into blastocysts, and germline-transmitted mice were established (Fig. 2C). The heterozygotes were fertile and appeared normal. Unlike the truncation null allele $Apc^{\Delta 716}$ (Oshima et al., 1995), the Apc^{neoR} heterozygotes developed only a few polyps in the intestines. Upon their heterozygous intercrosses, however, no homozygous pups were born (Table 1). We then examined the embryos derived from the heterozygous Apc^{neoR} intercrosses, but could not find obvious morphological abnormalities at 6.5 dpc (data not shown). At 7.5 dpc, however, the homozygous embryos showed a constricted appearance at the border between the embryonic and extraembryonic portions (Fig. 3A). At 8.5 dpc, every homozygous embryo showed an abnormal anterior region which was displaced outside the yolk sac (Fig. 3B and C). At 9.5 dpc, the homozygous embryos remained unturned (Fig. 3D). In addition, the anterior and ventral regions were abnormal in the homozy-

gotes (Fig. 3B–D; see below). Because the embryos homozygous for the Apc^{min}, $Apc^{\Delta 716}$, or Apc^{lacZ} alleles become abnormal around 5.5 dpc before gastrulation (Moser et al., 1995; Oshima et al., 1995; and data not shown), Apc^{neoR} appears to be a hypomorphic allele.

Attenuated expression from the Apc^{neoR} allele

Insertion of the PGK-*neo* cassette into an intron by homologous recombination can alter or disrupt the gene expression leading to a hypomorphic or null allele (reviewed in Lewendoski, 2001). Accordingly, the levels of *Apc* mRNA were estimated by using quantitative RT-PCR (TaqMan). As shown in Fig. 2D, the heterozygous and homozygous Apc^{neoR} embryos at 8.5 dpc expressed *Apc* mRNA at about 55 and 20% levels of the wild-type embryos, respectively. The results were consistent with those by semiquantitative RT-PCRs with several primers in different exons (data not shown, see Materials and methods). Because it was reported that the *neo* cassette contained cryptic splice sites (Jacks et al., 1994; Carmeliet et al., 1996), we examined the Apc^{neoR} transcripts for various segments between exons 11 and 15 by RT-PCR. However, only the normal splicing products that removed the *loxP* and PGK-*neo* cassettes were found, without any aberrantly spliced mRNA. We did not find any difference in the mRNA levels among exons either (data not shown, see Materials and methods).

It was conceivable that the *neo* cassette placed in the reverse orientation produced antisense RNA complementary to the *Apc* transcript. Such an example was suggested for the difference between Apc^{1638N} and Apc^{1638T} mutant mice (Fodde et al., 1996; Smits et al., 1999). To examine the possibility, we constructed an *Apc* allele with the *neo* cassette placed in the forward orientation at the same site as in the Apc^{neoR} allele (Apc^{neoF} allele, F for the forward orientation). Interestingly, embryos with the homozygous Apc^{neoF} allele showed the same phenotype as the homozygous Apc^{neoR} embryos (data not shown). Accordingly, the decrease in the Apc^{neoR} mRNA was most likely due to a promoter attenuation caused by insertion of the *loxP*-PGK-*neo* cassette into an enhancer site in intron 13.

To analyze expression of Apc protein from the Apc^{neoR} allele, we generated homozygous Apc^{neoR} ES cells (Fig. 4A) by selecting clones from the heterozygous Apc^{neoR} ES cells with a higher concentration of geneticin. A Western analysis showed that homozygous Apc^{neoR} ES cells expressed the full-length Apc protein. The levels in the heterozygous and homozygous ES cells were about 60 and 20% of the wild-type level, respectively (Fig. 4B). These results confirmed that the Apc^{neoR} is a hypomorphic allele whose expression is attenuated by ~80%. Because Apc functions in the Wnt signaling pathway by downregulating β-catenin, we next examined the stabilization of β-catenin in the homozygous Apc^{neoR} ES cells. For this purpose, we used a monoclonal antibody that recognizes nuclear (dephospho-) β-catenin (Schmelz et al., 2001) for Western immunoblotting. As shown in Fig. 4C, the protein levels in the heterozygous and homozygous ES cells were increased to about 1.1 and 2.8 times of the wild type, respectively. To examine whether this stabilization of β-catenin could increase the Wnt signaling activity, we performed transient transfections with luciferase reporter constructs controlled by TOPFLASH (Tcf binding motifs) and FOPFLASH (mutant motifs), respectively (Korinek et al., 1997). In the homozygous Apc^{neoR} ES cells, the TOPFLASH reporter activity was 7 times higher than that of the FOPFLASH. In the truncated mutant $Apc^{\Delta 716}$ homozygous ES cells, the transcriptional activity of TOPFLASH was about 40 times higher than that of FOPFLASH (Fig. 4D). These results indicate that attenuation of Apc expression causes an accumulation of the transcriptionally active nuclear β-catenin, resulting in the stimulation of the Wnt signaling pathway.

Anterior truncation in the Apc^{neoR} homozygote

In the homozygous Apc^{neoR} embryos, the head folds were missing and the brain was poorly formed, although some neural ectoderm was observed (compare Fig. 3G with H). To characterize these anterior defects in more detail, expression of several marker genes was determined by whole-mount in situ hybridization (Fig. 5). When 8.5-dpc embryos were hybridized with a probe for *Six3*, a forebrain marker (Fig. 5A; Oliver et al., 1995), no staining was found in the homozygous embryo (Fig. 5B). Likewise, the homozygous embryo was not stained with a probe for *Otx2* (Fig. 5D), a forebrain and midbrain marker (Fig. 5C; Simeone et al., 1993). Little hybridization was detected in the homozygous embryo with a probe for *Wnt1* (Fig. 5F) that is excluded from the forebrain but present in the midbrain and the dorsal aspect of the hindbrain (Fig. 5G; Parr et al., 1993). When the homozygous embryo was hybridized with a probe for *Hoxb1*, a rhombomere 4 marker in the hindbrain (Fig. 5G), staining was very weak and diffuse in the hindbrain, although strong staining remained in the caudal regions corresponding to the branchial arch and somitic mesoderm (Fig. 5H). Upon staining with a probe for *Egr2* (*Krox-20*), a marker for the presumptive rhombomeres 3 and 5 (Fig. 5I; Wilkinson et al., 1989), only one region was stained in the homozygous embryos (Fig. 5J). These results indicate that the homozygous Apc^{neoR} embryo lacks the forebrain and midbrain, but retains a portion of the hindbrain; i.e., its brain is truncated in the anterior hindbrain or caudal midbrain.

Defective formation of the visceral endoderm and axial mesendoderm in the Apc^{neoR} homozygote

The constriction at the embryonic–extraembryonic junction of the homozygous Apc^{neoR} embryo at 7.5 dpc (Fig. 3A) was very similar to that observed in the mutants of *Foxa2* (Ang and Rossant, 1994; Weinstein et al., 1994), *Lim1* (Shawlot and Behringer, 1995), *Otx2* (Acampora et al.,

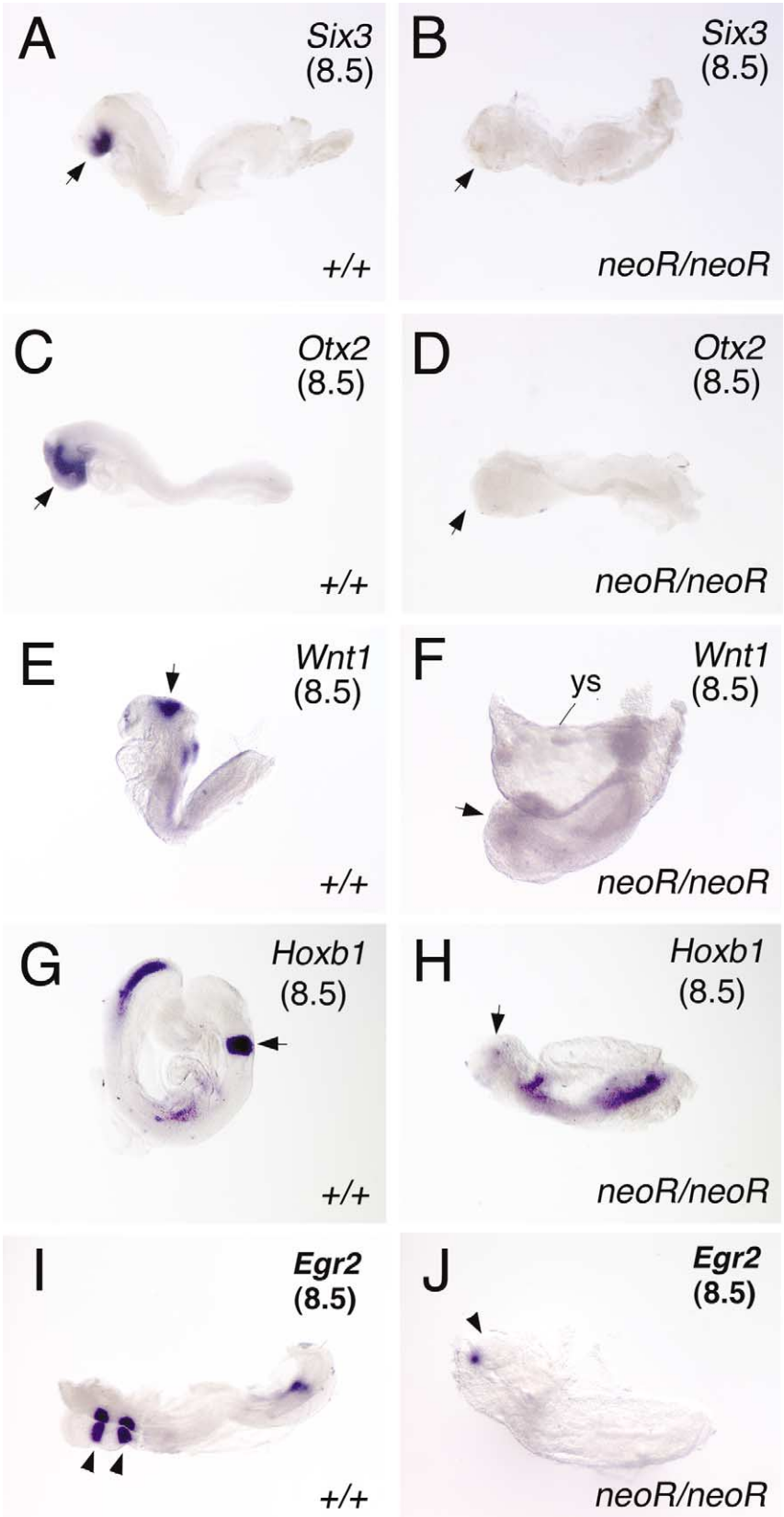

Fig. 5. Anterior truncation in the homozygous Apc^{neoR} embryos. Genotypes are: +/+, wild type (A, C, E, G, and I); and *neoR/neoR*, homozygous Apc^{neoR} (B, D, F, H, and J). (A, B) Whole-mount in situ hybridization at 8.5 dpc with a probe for *Six3*, a forebrain marker. (C, D) Embryos at 8.5 dpc stained with a probe for *Otx2*, forebrain, and midbrain marker. (E, F) Embryos at 8.5 dpc stained with a probe for *Wnt1*, a midbrain marker. Note that little staining is found in the homozygous mutant embryo compared with either of these three markers (arrows). (G, H) Embryos at 8.5 dpc stained with a probe for *Hoxb1*, a hindbrain marker. Note that weak and diffused staining is found in the anterior region of the homozygous mutant embryo compared with the wild type stained in rhombomere 4 (arrows). (I, J) Embryos at 8.5 dpc stained with a probe for *Egr2 (Krox-20)*, a hindbrain marker. Note a small stained spot in the homozygous mutant embryo (arrowhead in J) compared with two obvious bands in the wild-type embryo, corresponding to the presumptive rhombomeres 3 and 5 (arrowheads in I).

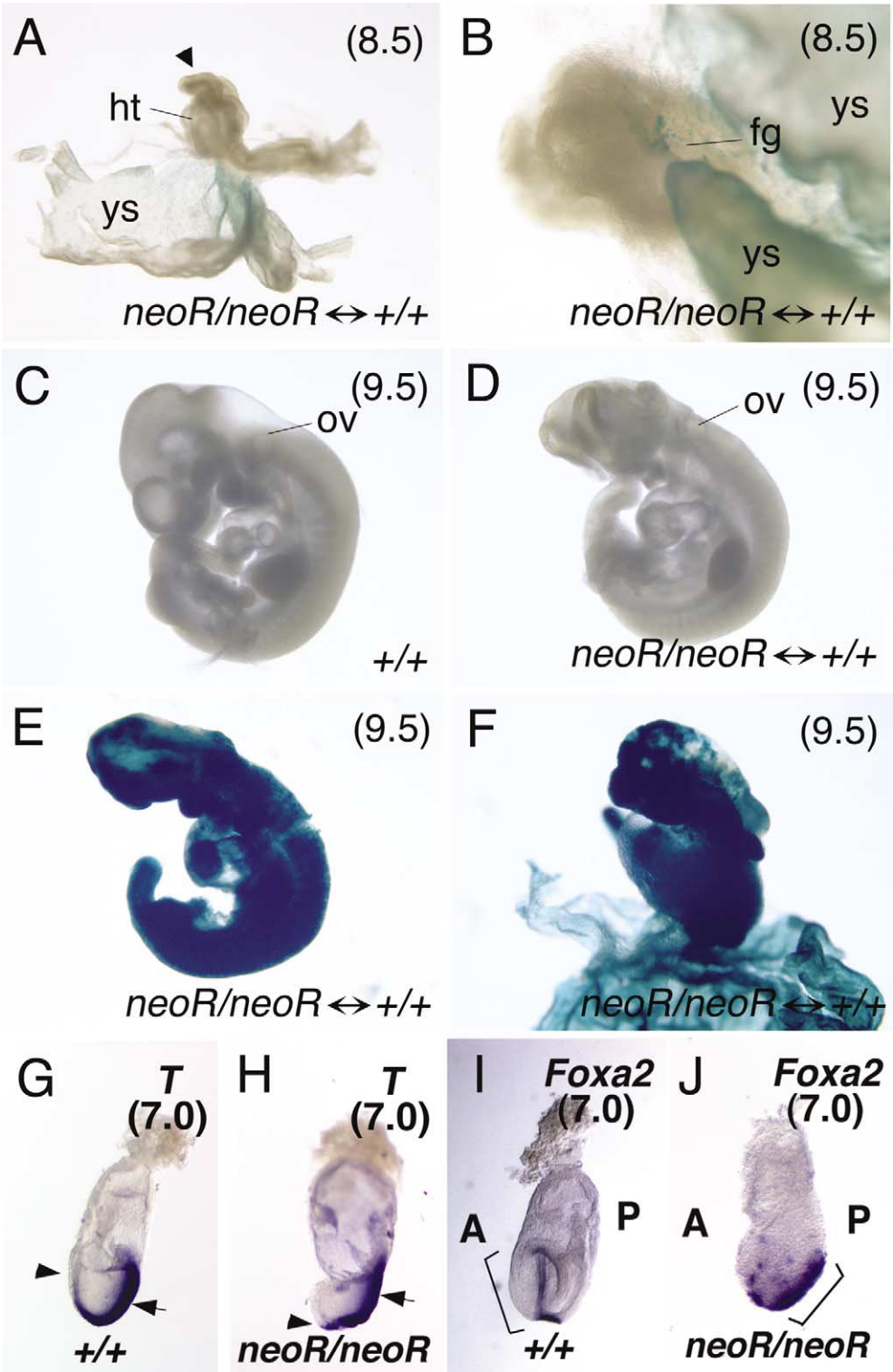

Fig. 6. Defective visceral endoderm and axial mesendoderm in the homozygous *Apc*^{neoR} embryos. (A–F) Chimeric embryos derived from the Rosa 26 blastocysts injected with the homozygous *Apc*^{neoR} ES cells (*neoR/neoR*↔+/+). (A, B) A strongly chimeric embryo at 8.5 dpc stained for β-galactosidase (lacZ). LacZ staining is seen in the yolk sac (ys) endoderm and definitive endoderm in the foregut (fg) and hindgut. In these chimeric embryos, ventral structures such as the heart (ht) and foregut were observed in the proper locations, although the head region was smaller than the wild type (arrowhead in A). (C) A nonchimeric control embryo showing the normal anterior neural development at 9.5 dpc. (D) A strongly chimeric embryo lacking anterior neural structures at 9.5 dpc. Note that turning of the embryo took place and ventral structures are normal. ov, otic vesicle. (E, F) Moderately chimeric embryos at 9.5 dpc. Note that anterior head structures are not developed well, although the homozygous *Apc*^{neoR} cells contributed to the anterior neural region. (G, H) Embryos at 7.5 dpc stained with a *T* probe. Note that *T* is expressed in the primitive streak (arrow), node, and head process (arrowhead) in the wild-type embryo. In the mutant embryo, *T* expression is found in the primitive streak (arrow) and node, but not extended to the anterior end of the embryo (arrowhead, the anterior end of the expressed tissue). (I, J) Embryos at 7.0 dpc stained for *Foxa2 (Hnf3b)* mRNA. Note that *Foxa2* is expressed in the node and head process in the wild-type embryo (bracket in I). In the mutant embryo, *Foxa2* is expressed in the posterior third of the embryo (bracket in J), but not in the head process.

1995; Matsuo et al., 1995; Ang et al., 1996), or *Nodal* (Varlet et al., 1997). These defects were caused by the abnormal anterior specification due to the impaired function of the anterior visceral endoderm (AVE). Recent studies suggested a significant role for the AVE in the anterior neural patterning (Beddington and Robertson, 1998, 1999). At the same time, it has also been suggested that the axial mesendoderm (AME) is required for the forebrain development (Tam and Steiner, 1999; Shawlot et al., 1999; Camus et al., 2000). Since *Apc* was expressed in all germ layers during gastrulation (Fig. 1), the lack of anterior neural structure in homozygous Apc^{neoR} embryos could be caused by defects in the AVE, AME, and/or anterior neural ectoderm (ANE) responding to their signals. To identify the tissues that require the *Apc* activity in the anterior neural structure formation, we constructed chimeric mouse embryos derived from the homozygous Apc^{neoR} ES cells injected into the Rosa26 blastocysts. Because injected ES cells do not contribute to the extraembryonic endoderm (Beddington and Robertson, 1989; Varlet et al., 1997), we took the advantage of this developmental bias to generate highly polarized chimeras in which the embryo proper was predominantly homozygous mutant for *Apc*, whereas the visceral endoderm was the wild type. The level of chimerism was analyzed by lacZ staining at 8.5–9.5 dpc. As expected, the wild-type cells were found in the endoderm of the visceral yolk sac and the definitive endoderm of the foregut and hindgut (Fig. 6A and B). In these chimeric embryos at 8.5 dpc, the head, foregut, and heart were found in the proper positions inside the yolk sac (Fig. 6A and B). Moreover, a head fold-like structure was formed and contained anterior brain tissues (Fig. 6A, arrowhead) that were missing in the homozygous Apc^{neoR} embryos (compared with Fig. 3B and D). However, the anterior neural plate in the chimeric embryos was developed less than in the wild-type embryos of the same stage (data not shown). By 9.5 dpc, however, the strongly chimeric embryos showed obvious defects in head development (Fig. 6D compared with C). These embryos lacked the anterior head structures. Even in moderately chimeric embryos (homozygous 25–50% Apc^{neoR} cells), the forebrain was smaller or abnormal (Fig. 6E and F). These results indicate that expression of Apc at the normal level is essential for anterior and ventral development of the mouse embryo in both the epiblast derivatives (AME and/or ANE) and visceral endoderm.

To further characterize the defects in the epiblast, we then determined expression of AME marker genes *T (Brachury)* and HNF3β (*Foxa2; Hnf3b*) in the homozygous Apc^{neoR} embryos. At 7.0 dpc, *T* is expressed in the node, head process, and primitive streak of the wild-type embryo (Wilkinson et al., 1990; Fig. 6G). In the homozygous embryos, *T* was expressed in the primitive streak, but its expression was not extended to the anterior side of the embryo (Fig. 6H). While HNF3β is expressed in the wild-type node, head process, and prechordal mesoderm (Sasaki and Hogan, 1993; Fig. 6I), it was not expressed in the homozygous Apc^{neoR} embryos in the tissues corresponding to the head process or prechordal mesoderm, although it was expressed in the posterior embryo (Fig. 6J). These results, taken together, suggest that the normal level of Apc expression is required for development of the functional AVE and AME, and that defective formation of AVE and AME by *Apc* attenuation causes anterior truncation in the homozygous embryos.

Partial axis duplication in the Apc^{neoR} homozygotes

At 8.5 dpc, ventral tissues such as the notochord and floor plate express sonic hedgehog (*Shh*) transcripts (Echelard et al., 1993). These midline structures appeared duplicated at the anterior end of the homozygous Apc^{neoR} embryo whose head fold was missing (Fig. 7A). In transverse sections, two regions were stained in the neural tube, indicating duplicated floor plate at the anterior end (arrowheads in Fig. 7B). To confirm this partial axis duplication, the embryos were stained for the *T (Brachury)* transcripts. Because *T* is expressed in the primitive streak and notochord in the wild-type embryo at 8.5 dpc (Willkinson et al., 1990; Fig. 7C), the branched notochordal staining at the anterior end confirmed the duplication of the notochord in the homozygous embryo (Fig. 7C and D).

Axis duplication can be induced experimentally in the gastrulating embryo by grafting the node, because the mouse node is equivalent to the Spemann's organizer in frogs (Beddington, 1994). Therefore, it is possible that expansion of the organizer activity in the node may have caused the partial axis duplication in the homozygous Apc^{neoR} embryo. To investigate this possibility, we determined expression of *Nodal* by in situ hybridization. In the wild-type embryo at 7.5 dpc, *Nodal* was expressed at the distal end of the embryo as described (Fig. 7E; Conlon et al., 1994). In the homozygote, however, its staining was not restricted to the distal end but distributed diffusely (Fig. 7E). At this stage, HNF3β was also expressed diffusely in the posterior embryo corresponding to the region of *Nodal* expression (Fig. 6J compared with I). These results indicate that the node in the homozygous Apc^{neoR} embryo is disorganized and expanded, which causes the secondary axis formation.

Abnormal ventral morphogenesis in the Apc^{neoR} homozygotes

At 9.5 dpc, *Shh* transcripts were found in the notochord, floor plate, brain, and gut in the wild-type embryos (Fig. 8A). In the Apc^{neoR} homozygotes, however, only the presumptive notochord and floor plate at the ventral midline were stained in the unturned embryo, without any staining for the anterior or ventral organs, such as the brain, heart, or foregut (Fig. 8B). To investigate the heart formation in detail, we used a probe for cardiac myosin heavy chain (MHC, *Myhca*) mRNA. Although the homozygous embryos

showed strong staining, it was not found in the ventral region as in the wild type (Fig. 8C and D). Rather, the heart tubes remained on the dorsal side of the unturned embryo and fused only partially as shown in a transverse section (Fig. 8E). The same pattern was obtained with a probe for cardiac troponin C as well (data not shown).

In the mouse embryo, the bilateral heart primordia migrate and fuse at the ventral midline, forming the single heart tube (Fig. 8F). Through this process, the foregut is also formed by closure of the definitive endoderm layer, and the anterior embryo is positioned inside the yolk sac. Accordingly, a defect in this process should result in bilateral heart tubes (cardia bifida), lack of the normal foregut, and failure of the anterior embryo to be enclosed by the yolk sac. Because the anterior and ventral regions of the homozygous Apc^{neoR} embryo remained outside the yolk sac, we then investigated whether this phenotype was caused by a defect in the process of ventral folding. We first examined the foregut cells with a gut-specific marker, HNF3α (*Foxa1*), which stained the foregut endoderm in the wild-type embryo (Fig. 8G and I). Although the gut-endoderm expressing HNF3α was found in the mutant, its expression was on the outside surface of the embryo, and no involuted foregut was formed (Fig. 8H, bracket, Fig. 8J). We then determined expression of *Gata4* in the homozygous Apc^{neoR} embryos. At 8.5 dpc in the wild-type embryo, it was expressed on the border between the definitive and visceral endoderm, corresponding to the anterior intestinal portal (AIP) (Fig. 8K). Interestingly, the mutant embryo expressed *Gata4* on the dorsal side (Fig. 8L). This result also showed that the border between the definitive and visceral endoderm was on the dorsal side, and the foregut was not formed properly.

As shown above (Fig. 6A–F), defects in the ventral morphogenesis were rescued in the strongly chimeric embryos derived from Rosa26 blastocysts injected with Apc^{neoR} ES cells. The heart and foregut were correctly positioned, despite the complete absence of the wild-type *Apc* cells in the splanchnic mesoderm derivatives. The anterior portion of the chimeric embryo was surrounded by the yolk sac by 8.5–9.5 dpc. These results indicate that the normal level Apc in the visceral endoderm and/or definitive endoderm can support proper ventral morphogenesis. These results collectively indicate that the defective lateral-to-ventral folding of the homozygous Apc^{neoR} embryos caused the abnormal placement of the anterior embryo outside the yolk sac, defective foregut formation, and failure of the cardiac mesoderm to fuse at the ventral midline (Fig. 8F).

Embryonic lethality of the double mutant $Apc^{neoR/lacZ}$

To investigate the effects of *Apc* attenuation further, we crossed the Apc^{neoR} heterozygotes with the Apc^{lacZ} mice. Apc^{lacZ} is a truncation null allele at codon 716, and its homozygotes become abnormal at the egg cylinder stage before 6.5 dpc, like in the $Apc^{\Delta 716}$ homozygotes (data not shown). Because the mRNA level of the Apc^{neoR} allele was attenuated by 80%, that of the $Apc^{neoR/lacZ}$ double mutant embryos was expected to be reduced to 10% of the wild type. In the double mutant embryos, the phenotypes were more severe than in the Apc^{neoR} homozygotes, but were milder than in the Apc^{lacZ} homozygotes (Fig. 9B). In the histological sections of the 6.5-dpc embryos, the embryonic ectodermal cells remained only in the distal region (Fig. 9B, arrow), although the visceral endodermal cells appeared unaffected (Fig. 9B, arrowhead). At 7.5 dpc, the embryonic region of the double mutant was protruding from the yolk sac (Fig. 9C), and this phenotype was more prominent at 8.5 dpc (Fig. 9D). These results show that most embryonic ectodermal cells of the $Apc^{neoR/lacZ}$ embryos become defective by 7.5 dpc.

Discussion

Because the *Apc* gene is expressed ubiquitously and the null homozygous mutants are lethal at an early embryonic stage, it has been difficult to determine its functions in the mouse embryo. To overcome such difficulties, it would be especially valuable if we have an allelic series ranging from the wild to null function. To this end, we constructed a novel hypomorphic *Apc* allele whose expression was attenuated by about 80%. Although a decrease in the *Apc* gene dosage to 50% in the $Apc^{\Delta 716}$ or Apc^{lacZ} heterozygotes did not cause any apparent developmental defects, a further decrease in the *Apc* expression to about 20% in the homozygous Apc^{neoR} embryo resulted in severe defects in early development. Furthermore, in the double mutant $Apc^{neoR/lacZ}$, whose *Apc* expression was expected to be about 10% of the wild type, the embryonic development was affected even more severely. Our results suggest that the cellular level of Apc protein functions as a quantitative regulator of the Wnt signaling.

In the mouse embryo, the Wnt signaling plays a key role in the anterior–posterior axial development (reviewed in Yamaguchi, 2001). Axis duplications have been reported in the homozygous *Axin (fused; Fu)* mutant embryos (Glucksohn-Shoenheimer, 1949; Jacob-Cohen et al., 1984; Perry et al., 1995; Zeng et al., 1997) and in the *Cwnt8C* misexpression transgenic mouse embryos (Pöpperl et al., 1997). On the other hand, neither the node nor the primitive streak is formed in the homozygous *Wnt3* knockout embryos (Liu et al., 1999), and the axis formation is defective in the β-catenin-deficient mouse embryos (Huelsken et al., 2000). The embryonic phenotypes of our homozygous Apc^{neoR} mutant are similar to those of one class of the *Cwnt8C* misexpression transgenic mutants (Pöpperl et al., 1997). The notochord extends closer to the anterior limit of the embryo, and shows partial axis duplication at 8.5 dpc. In addition to the truncated neural folds, formation of the foregut is also disrupted. Although abnormal heart development was mentioned, no marker studies were presented. It is therefore possible that the heart tubes remained in the dorsal side, like

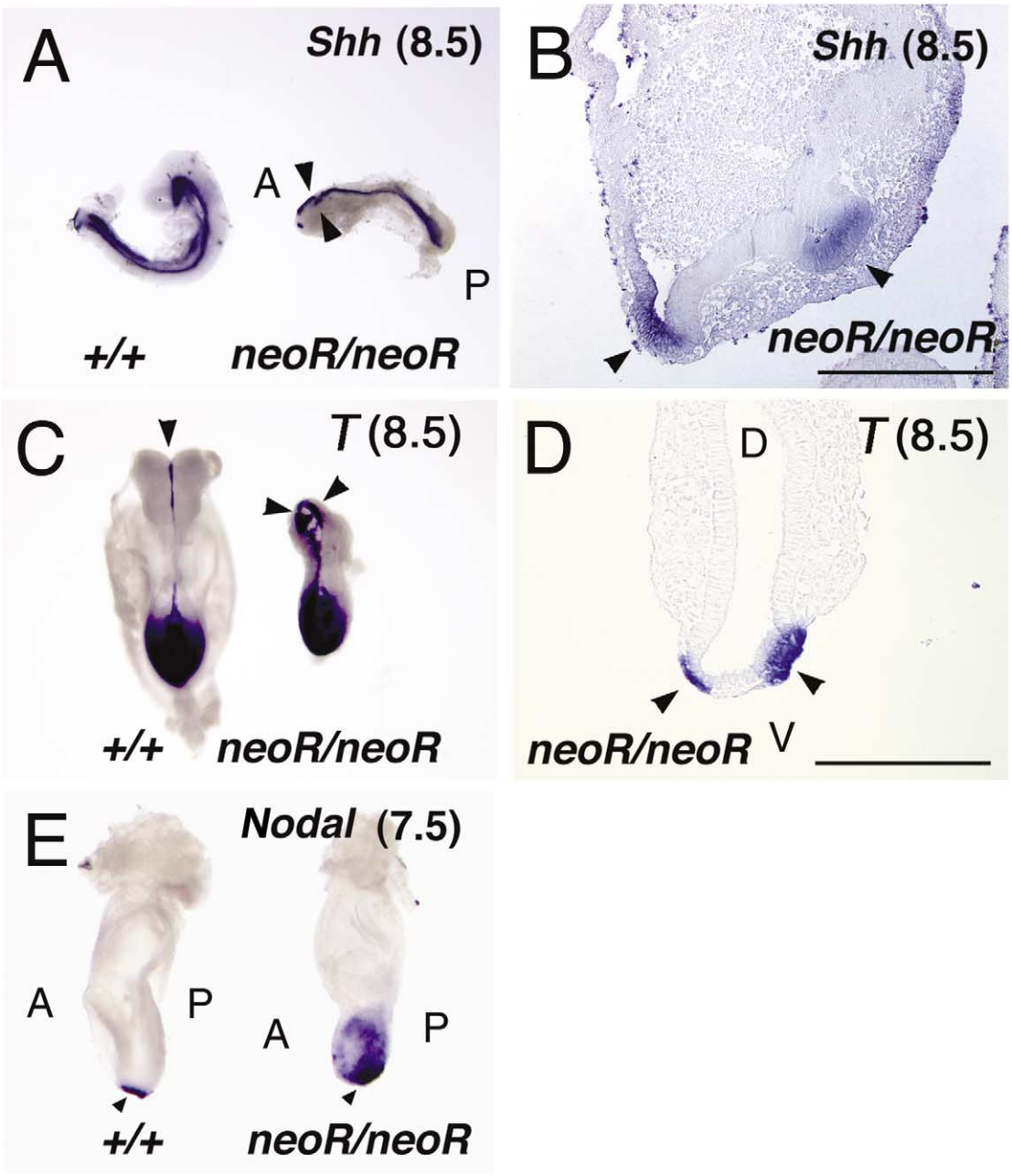

Fig. 7. Partial axis duplication in the homozygous Apc^{neoR} embryos. (A) Embryos at 8.5 dpc stained with a probe for *Shh*. Note the branched neural tube at the anterior end of the homozygous embryo (*neoR/neoR*, arrowheads). (B) A transverse section of the homozygous Apc^{neoR} embryo stained with the *Shh* probe shown in (A). Note that the duplicated floor plate (arrowhead) is stained. (C) Embryos at 8.5 dpc stained with a probe for *T*. Note the branched notochord (arrowheads) at the anterior end. (D) A transverse section of the homozygous Apc^{neoR} embryo stained with the *T* probe shown in (A). Note that the duplicated notochord (arrowheads) is stained. (E) Embryos at 7.5 dpc stained for the *Nodal* mRNA. Note the diffuse staining in the homozygous mutant. Magnification bars in (B) and (D), 500 μm.

in our homozygous Apc^{neoR} embryos. Recently, it has been reported that anteriorly localized Wnt antagonist *Dkk1* is critical for inducing anterior structures in the mouse embryo (Mukhopadhyay et al., 2001). These data also indicate that adequate suppression of the Wnt signaling is necessary for proper anterior development. The phenotypes of our *Apc* hypomorphic mutant embryos are consistent with such regulation mechanisms of the Wnt signaling pathway.

Anterior defects which are similar to those in our homozygous Apc^{neoR} embryos have been reported also in the *Otx2*, *Hnf3β*, and *Lhx1* homozygous embryos, respectively (Acampora et al., 1995; Ang et al., 1996; Matsuo et al., 1995; Ang and Rossant, 1994; Shawlot and Behringer, 1995). In these mutant embryos, lack of the forebrain is found early in gastrulation because of a failure in the induction of the anterior neural plate. In the forebrain devel-

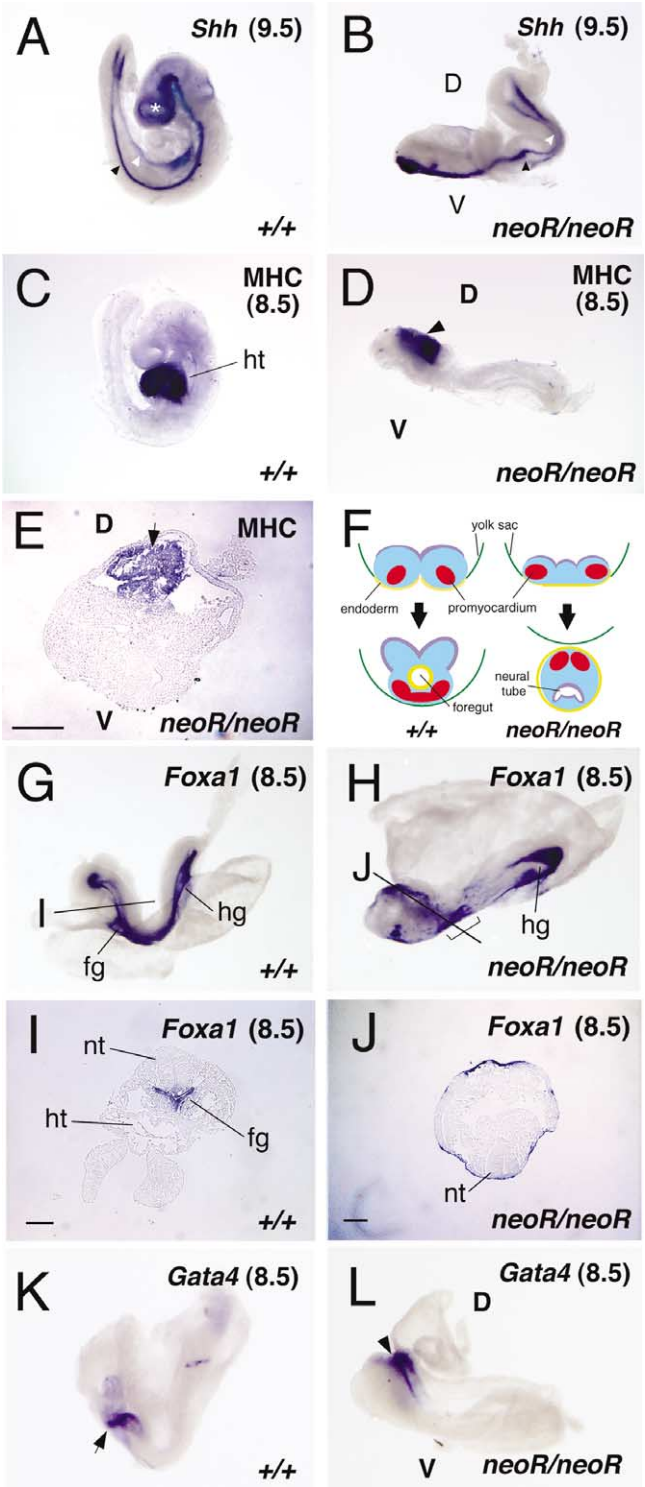

Fig. 8. Defective ventral morphogenesis in the homozygous Apc^{neoR} embryos. Genotypes are: +/+, wild type; and *neoR/neoR*, homozygous Apc^{neoR}. (A, B) Embryos at 9.5 dpc stained with a probe for *Shh*. Note that the floor plate (black arrowheads), brain (white asterisk), and gut (white arrowhead) are visible in the wild-type littermate, whereas only the presumptive floor plate (black arrowhead) and hindgut (white arrowheads) are stained in the mutant. (C, D) Embryos at 8.5 dpc stained with a probe for myosin heavy chain (MHC, *Myhca*), a heart marker. Note that the heart precursors exist in the homozygous embryo, but remain on the dorsal ridge of the unturned embryo (arrowhead), whereas the heart is formed on the ventral side in the wild-type embryo (ht). (E) A transverse section through the heart precursor of the MHC-stained mutant embryo in (D). Note the incomplete heart tubes, fused partially on the dorsal side (arrow). (F) An illustration showing the relationship between the neuroectoderm (neural tube in gray), heart precursors (promyocardium in red), and gut endoderm (yellow). (G, H) Embryos at 8.5 dpc stained for the HNF3α (*Foxa1*) mRNA. Note that the foregut is absent in the homozygous embryo, but the stained endoderm cells expand on the surface of the embryo (bracket). (I, J) Transverse sections through the HNF3α-stained region of the embryo in (G) and (H) (through lines I and J, respectively). Note that involuted foregut was not found in the homozygous mutant. (K, L) Embryos at 8.5 dpc stained for the *Gata4* mRNA. Note that the expression in the wild type is at the AIP, whereas it is expressed on the dorsal side in the homozygous mutant (arrowheads). The embryonic polarities are shown by: D, dorsal; and V, ventral. The organs are abbreviated as: fg, foregut; hg, hindgut; ht, heart; and nt, neural tube. Magnification bars in (E), (I), and (J), 250 μm.

opment, the AVE is proposed to play a central role as a head organizer (Thomas and Beddington, 1996; Beddington and Robertson, 1999). Chimeric studies of *Nodal*, *Otx2*, *Hnf3β*, and *Lim1* mutants have suggested that the visceral endoderm is essential for the forebrain formation (Varlet et al., 1997; Rhinn et al., 1998; Dufort et al., 1998; Shawlot et al., 1999). On the other hand, recent transplantation studies have suggested that the AVE alone cannot induce the anterior neuroectoderm (Tam and Steiner, 1999). Furthermore, it is also suggested that the AME is required in the forebrain development by chimeric studies of *Lhx1* embryos and surgical removal experiments (Shawlot et al., 1999; Camus et al., 2000). Our chimera studies demonstrate that the normal level of Apc in the visceral endoderm rescued only partially the development of the homozygous Apc^{neoR} anterior neural ectoderm. Interestingly, differentiation of the AME that should express *T* and HNF3β was defective in the Apc^{neoR} homozygotes. These results collectively indicate that Apc is required for the function of not only AVE but also AME and/or ANE.

The ventral morphogenesis in the mouse embryos is initiated by a rostral-to-caudal and lateral-to-ventral displacement of the embryonic mesoderm subjacent to the headfolds, which eventually fuse at the ventral midline and form a linear heart tube (Kaufman, 1992). Concomitant with these cell movements, the anteriormost definitive endoderm involutes to form the foregut pocket that is subsequently extended caudally during the midgut specification. In the homozygous Apc^{neoR} mutant, the definitive endoderm cells expressing *Foxa1* at 8.5 dpc were differentiated properly, although tubular foregut was not formed. In contrast, chimeric embryos in which the wild-type cells populated only in the endoderm did not exhibit abnormalities in development of the ventral structures. Thus, we conclude that presence of the wild-type cells in the visceral endoderm and/or definitive endoderm is sufficient to induce normal ventral development. These results suggest that Apc plays a critical role in the ventral folding processes by regulating the endodermal cell movement. Although the mechanisms responsible for the cell migration, growth, and patterning of

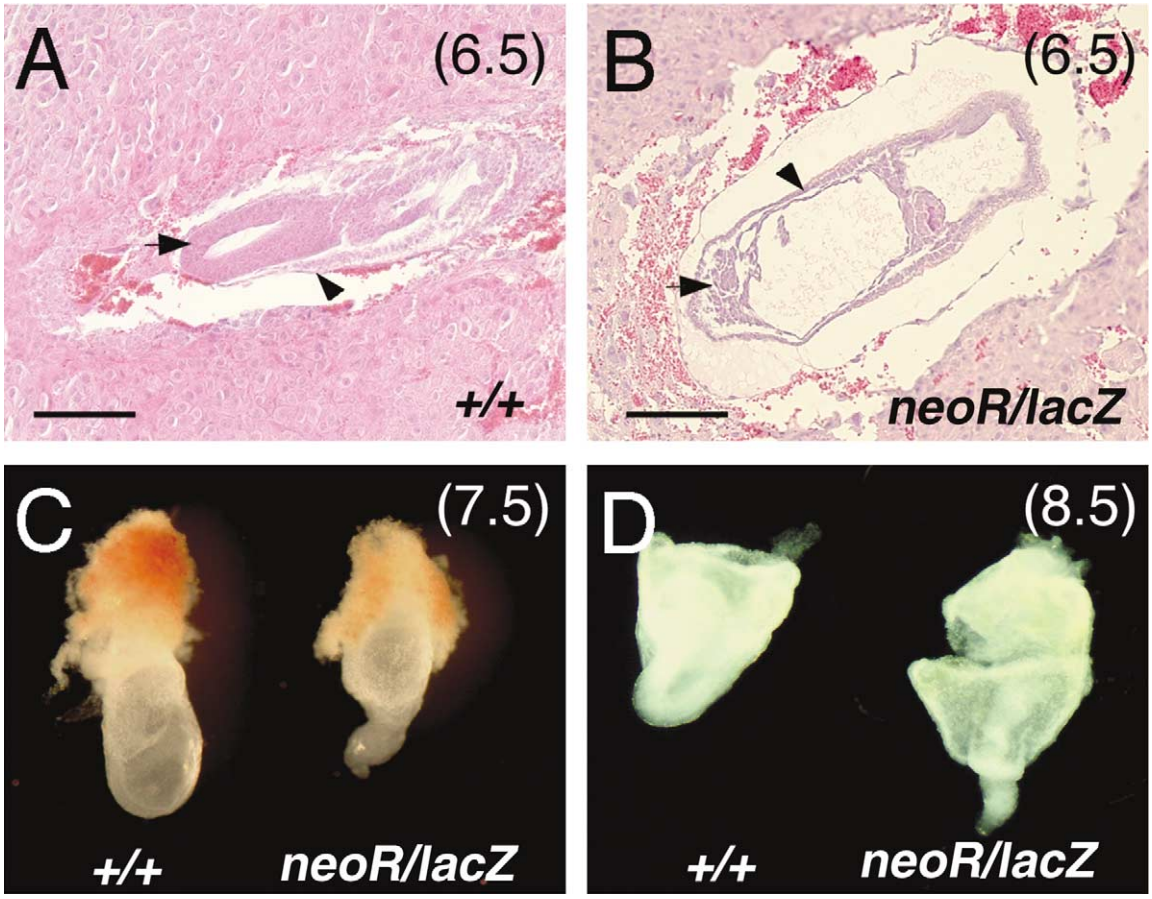

Fig. 9. Defects in the *Apc*$^{neoR/lacZ}$ double mutant embryos. Genotypes are: (+/+), wild type; and (*neoR/lacZ*), double mutant *Apc*$^{neoR/lacZ}$. (A) A longitudinal section of a wild-type embryo (a littermate of that in B) in utero at 6.5 dpc. (B) A longitudinal section of a double mutant embryo in utero at 6.5 dpc. Note that the visceral endoderm appears normal (arrowhead) but the embryonic ectoderm is defective (arrow). (C) A double mutant embryo compared with the wild type at 7.5 dpc. (D) A double mutant embryo compared with the wild type at 8.5 dpc. Note the protruding anterior embryo from the yolk sac. (A, B) Histological sections (H&E). Magnification bars, 100 μm. (C, D) Dissection micrographs.

the ventral structures remain largely unknown, the *Gata4* gene is one of the candidates involved in these processes (Kuo et al., 1997; Molkentin et al., 1997). In the Apc hypomorphic embryos, however, the *Gata4* expression was not reduced. It is conceivable that Apc itself plays a mechanical role in the ventral folding, because Apc is also implicated in the cell migration (Nathke et al., 1996; Pollack et al., 1997). Alternatively, Wnt signaling may regulate expression of certain genes in the endoderm required for the ventral folding processes.

In the *Apc*$^{neoR/lacZ}$ double mutant embryos, more severe phenotypes were observed than in the homozygous *Apc*^{neoR} embryos. The epiblast remained only at the distal end of the embryo, and the neuroectoderm was hardly developed. The homozygous *Apc* null embryos, such as *Apc*^{Min}, *Apc*$^{\Delta 716}$, or *Apc*^{lacZ}, die much earlier before the gastrulation due to degeneration of the entire epiblast cells (Moser et al., 1995; Oshima et al., 1995; data not shown). These results indicate a dose-dependent regulation by Apc of the epiblast development in the mouse embryo.

In conclusion, we have demonstrated that an *Apc* hypomorphic allele causes anterior truncation, partial axis duplication, and defects in the ventral morphogenesis.

Acknowledgments

We thank N. Murai, R. Nakajima, J. Inuzuka, and N. Matsuda for excellent technical assistance, H. Miyoshi for cells, and I. Dawid, J. Wells, Y. Saga, N. Harada, and K. Takaku for helpful discussions and comments. This work was supported in part by the Joint Research Fund between the University of Tokyo and Banyu Pharmaceutical Co.; and Grants from Monbusho (MESSC) and Organization for Pharmaceutical Safety and Research (OPSR), Japan (to M.M.T.).

References

Acampora, D., Mazan, S., Lallemand, Y., Avantaggiato, V., Maury, M., Simeone, A., Brulet, P., 1995. Forebrain and midbrain regions are

deleted in *Otx2*$^{-/-}$ mutants due to a defective anterior neuroectoderm specification during gastrulation. Development 121, 3279–3290.

Acampora, D., Avantaggiato, V., Tuorto, F., Briata, P., Corte, G., Simeone, A., 1998. Viceral endoderm-restricted translation of *Otx*1 mediates recovery of *Otx*2 requirements for specification of anterior neural plate and normal gastrulation. Development 125, 5091–5104.

Ang, S.-L., Rossant, J., 1994. *HNF-3β* is essential for node and notochord formation in mouse development. Cell 78, 561–574.

Ang, S.-L., Jin, O., Rhinn, M., Daigle, N., Stevenson, L., Rossant, J., 1996. A target mouse *Otx2* mutation leads to severe defects in gastrulation and formation of axial mesoderm and to deletion of rostral brain. Development 122, 243–252.

Beddington, R.S.P., 1994. Induction of a second neural axis by the mouse node. Development 120, 613–620.

Beddington, R.S.P., Robertson, E.J., 1989. An assessment of the developmental potential of embryonic stem cells in the midgestation of embryo. Development 105, 733–737.

Beddington, R.S.P., Robertson, E.J., 1998. Anterior patterning in mouse. Trends Genet. 14, 277–284.

Beddington, R.S.P., Robertson, E.J., 1999. Axis development and early asymmetry in mammals. Cell 96, 195–209.

Bienz, M., Clevers, H., 2000. Linking colorectal cancer to Wnt signaling. Cell 103, 311–320.

Camus, A., Davidson, B.P., Billiards, S., Khoo, P., Rivera-Perez, J.A., Wakamiya, M., Behringer, R.R., Tam, P.P., 2000. The morphogenetic role of midline mesendoderm and ectoderm in the development of the forebrain and the midbrain of the mouse embryo. Development 127, 1799–1813.

Carmeliet, P., Ferreira, V., Breier, G., Pollefeyt, S., Kieckens, L., Gertsenstein, M., Fahrig, M., Vandenhoeck, A., Harpal, K., Eberhardt, C., Declercq, C., Pawling, J., Moons, L., Collen, D., Risau, W., Nagy, A., 1996. Abnormal blood vessel development and lethality in embryos lacking a single VEGF allele. Nature 380, 435–439.

Conlon, F.L., Lyons, K.M., Takaesu, N., Barth, K.S., Kispert, A., Hermann, B., Robertson, E.J., 1994. A primary requirement for nodal in the formation and maintenance of the primitive streak in the mouse. Development 120, 1919–1928.

Dufort, D., Schwarts, L., Harpal, K., Rossant, J., 1998. The transcription factor HNF3*β* is required in visceral endoderm for normal primitive streak morphogenesis. Development 125, 3015–3025.

Echelard, Y., Epstein, D.J., St-Jacques, B., Shen, L., Mohler, J., McMahon, J.A., McMahon, A.P., 1993. Sonic hedgehog, a member of a family of putative signaling molecules, is implicated in the regulation of CNS polarity. Cell 75, 1417–1430.

Fodde, R., Edelmann, W., Yang, K., van Leeuwen, C., Carlson, C., Renault, B., Breukel, C., Alt, E., Lipkin, M., Khan, P.M., Kucherlapati, R., 1994. A targeted chain-termination mutation in the mouse *Apc* gene results in multiple intestinal tumors. Pro. Natl. Acad. Sci. USA 91, 8969–8973.

Gluecksohn-Schoenheimer, S., 1949. The effects of a lethal mutation responsible for duplications and twinning in mouse embryos. J. Exp. Zool. 110, 47–76.

Groden, J., Thliveris, A., Samowitz, W., Carlson, M., Gelbert, L., Albertsen, H., Joslyn, G., Stevens, J., Spirio, L., Robertson, M., et al., 1991. Identification and characterization of the familial adenomatous polyposis coli gene. Cell 66, 589–600.

Huelsken, J., Vogel, R., Brinkmann, V., Erdmann, B., Birchmeier, C., 2000. Requirement for *β*-catenin in anterior–posterior axis formation in mice. J. Cell Biol. 148, 567–578.

Jacks, T., Shih, T.S., Schmitt, E.M., Bronson, R.T., Bernards, A., Weinberg, R.A., 1994. Tumour predisposition in mice heterozygous for a targeted mutation in Nf1. Nat. Genet. 3, 353–361.

Jacobs-Cohen, R.J., Spiegelman, M., Cookingham, J.C., Bennett, D., 1984. Knobbly, a new dominant mutation in the mouse that affects embryonic ectoderm organization. Genet. Res. 43, 43–50.

Kaufman, M.H., 1992. The Atlas of Mouse Development. Academic Press, London.

Kinzler, K.W., Nilbert, M.C., Su, L.K., Vogelstein, B., Bryan, T.M., Levy, D.B., Smith, K.J., Preisinger, A.C., Hedge, P., McKechnie, D., et al., 1991. Identification of FAP locus genes from chromosome 5q21. Science 253, 661–665.

Korinek, V., Barker, N., Morin, P.J., van Wichen, D., de Weger, R., Kinzler, K.W., Vogelstein, B., Clevers, H., 1997. Constitutive transcriptional activation by a *β*-catenin-Tcf complex in APC$^{-/-}$ colon carcinoma. Science 275, 1784–1787.

Kuo, C.T., Morrisey, E.E., Anandappa, R., Sigrist, K., Lu, M.M., Parmacek, M.S., Soudais, C., Leoden, J.M., 1997. GATA4 transcription factor is required for ventral morphogenesis and heart tube formation. Genes Dev. 11, 1048–1060.

Lewandoski, M., 2001. Conditional control of gene expression in the mouse. Nat. Rev. Genet. 2, 743–755.

Liu, P., Wakamiya, M., Shea, M.J., Albrecht, U., Behringer, R.R., Bradley, A., 1999. Requirement for *Wnt3* in vertebrate axis formation. Nat. Genet. 22, 361–365.

Matsuo, I., Kuratani, S., Kimura, C., Takeda, N., Aizawa, S., 1995. Mouse Otx2 functions in the formation and pattering of rostral head. Genes Dev. 9, 2646–2658.

Molkentin, J.D., Lin, Q., Duncan, S.A., Olson, E.N., 1997. Requirement of the transcriptional factor GATA4 for heart tube formation and ventral morphogenesis. Genes Dev. 11, 1061–1072.

Mortensen, R.M., Conner, D.A., Chao, S., Geisterfer-Lowrance, A.A., Seideman, J.G., 1992. Production of homozygous mutant ES cells with a single targeting construct. Mol. Cell. Biol. 12, 2391–2395.

Moser, A.R., Shoemaker, A.R., Connely, C.S., Clipson, L., Gould, K.A., Luongo, C., Dove, W.F., Siggers, P.H., Gardner, R.L., 1995. Homozygosity for the Min allele of Apc results in disruption of mouse development prior to gastrulation. Dev. Dyn. 203, 422–433.

Mukhopadhyay, M., Shtrom, S., Rodriguez-Esteban, C., Chen, L., Tsukui, T., Gomer, L., Dorward, D.W., Glinka, A., Grinberg, A., Huang, S.-P., Niehrs, C., Belmonte, J.C.I., Westphal, H., 2001. *Dickkopf1* is required for embryonic head induction and Limb morphogenesis in the mouse. Dev. Cell 1, 423–434.

Nathke, I.S., Adams, C.L., Polakis, P., Sellin, J.H., Nelson, W.J., 1996. The adenomatous polylosis coli tumor suppressor protein localizes to plasma membrane sites involved in active cell migration. J. Cell Biol. 134, 165–179.

Nusse, R., 1997. A versatile transcriptional effector of Wingless signaling. Cell 89, 321–323.

Oliver, G., Mailhos, A., Wehr, R., Copeland, N.G., Jenkins, N.A., Gruss, P., 1995. *Six3* a murine homologue of the *sine oculis* gene, demarcates the most anterior border of the developing neural plate and is expressed during eye development. Development 121, 4045–4055.

Oshima, M., Oshima, H., Kitagawa, K., Kobayashi, M., Itakura, C., Taketo, M., 1995. Loss of Apc heterozygosity and abnormal tissue building in nascent intestinal polyps in mice carrying a truncated Apc gene. Proc. Natl. Acad. Sci. USA 92, 4482–4486.

Parr, B.A., Shea, M.J., Vassileva, G., McMahon, A.P., 1993. Mouse Wnt genes exhibit discrete domains of expression in the early embryonic CNS and limb buds. Development 119, 249–261.

Perry, W.L., III, Vasicek, T.J., Lee, J.J., Rossi, J.M., Zeng, L., Zhang, T., Tilghman, S.M., Constantini, F., 1995. Phenotypic and molecular analysis of a transgenic insertional allele of mouse Fused locus. Genetics 141, 321–332.

Polakis, P., 1999. The oncogenic activation of *β*-catenin. Curr. Opin. Genet. Dev. 9, 15–21.

Polakis, P., 2000. Wnt signaling and cancer. Genes Dev. 14, 1837–1851.

Pollack, A.L., Barth, A.I.M., Altschuler, Y., Nelson, W.J., Mostov, K.E., 1997. Dynamics of *β*-catenin interactions with APC protein regulate epithelial tubulogenesis. J. Cell Biol. 137, 1651–1662.

Pöpperl, H., Schmidt, C., Wilson, V., Hume, C.R., Dodd, J., Krumlauf, R., Beddington, R.S.P., 1997. Misexpression of Cwnt8C in the mouse induces an ectopic embryonic axis and causes a truncation of the anterior neuroectoderm. Development 124, 2997–3005.

Rhinn, M., Dierich, A., Shawlot, W., Behringer, R.R., Le Meur, M., Ang, S.-L., 1998. Sequential roles for *Otx2* in viceral endoderm and neuroectoderm for forebrain and midbrain induction and specification. Development 125, 845–856.

Saga, Y., Hata, N., Kobayashi, S., Magnuson, T., Seldin, M.F., Taketo, M.M., 1996. MesP1: a novel basic helix–loop–helix protein expressed in the nascent mesodermal cells during mouse gastrulation. Development 122, 2769–2778.

Sasaki, H., Hogan, B.L.M., 1993. Differential expression of multiple folk head related genes during gastrulation and axial pattern formation in the mouse embryo. Development 118, 47–59.

Shawlot, W., Wakamiya, M., Kwan, K.M., Kania, A., Jessell, T.M., Behringer, R.R., 1999. Lim1 is required in both primitive streak-derived tissues and visceral endoderm for head formation in the mouse. Development 126, 4925–4932.

Shawlot, W., Behringer, R.R., 1995. Requirement for Lim1 in head-organizer function. Nature 374, 425–430.

Schmelz, E.M., Roberts, P.C., Kustin, E.M., Lemonnier, L.A., Sullards, M.C., Dillehay, D.L., Merrill, A.H., Jr., 2001. Modulation of intracellular β-catenin localization and intestinal tumorigenesis in vivo and in vitro by sphingolipids. Cancer Res. 61, 6723–6729.

Simeone, A., Acampora, D., Mallamaci, A., Stornaiuolo, A., D'Apice, M.R., Nigro, V., Boncinelli, E., 1993. A vertebrate gene related to orthodenticle contains a homeodomain of the bicoid class and demarcates anterior neuroectoderm in the gastrulating mouse embryo. EMBO J. 12, 2735–2747.

Smits, R., Kielman, M., Breukel, C., Zucher, C., Neufeld, K., Jagmohan-Changur, S., Hofland, N., van Dijk, J., White, R., Edelmann, W., Kucherlapati, R., Khan, P.M., Fodde, R., 1999. *Apc*1638T: a mouse model delineating critical domains of the adenomatous polyposis coli protein involved in tumorigenesis and development. Genes Dev. 13, 1309–1321.

Tam, P.L., Steiner, K.A., 1999. Anterior patterning by synergistic activity of the early gastrula organizer and the anterior germ layer tissues of the mouse embryo. Development 126, 5171–5179.

Thomas, P., Beddington, R.S.P., 1996. Anterior primitive endoderm may be responsible for patterning their anterior neural plate in the mouse embryo. Curr. Biol. 6, 1487–1496.

Varlet, I., Collignon, J., Robertson, E.J., 1997. Nodal expression in the primitive endoderm is required for specification of the anterior axis during mouse gastrulation. Development 124, 1033–1044.

Weinstein, D.C., Ruiz, I., Altaba, A., Chen, W.S., Hoodless, P., Prezioso, V.R., Jessel, T.M., Darnell, J.E., 1994. The winged-helix transcription factor HNF-3beta is required for notochord development in the mouse embryo. Cell 78, 575–588.

Wilkinson, D.G., Bhatt, S., Chavrier, P., Bravo, R., Charnay, P., 1989. Segment-specific expression of a zinc-finger gene in the developing nervous system of the mouse. Nature 337, 461–464.

Wilkinson, D.G., Bhatt, S., Herrmann, B.G., 1990. Expression pattern of the mouse T gene and its role in mesoderm formation. Nature 343, 657–659.

Wodarz, A., Nusse, R., 1998. Mechanisms of Wnt signaling in development. Annu. Rev. Cell Dev. Biol. 14, 59–88.

Yamaguchi, T.P., 2001. Heads or tails: Wnts and anterior-posterior patterning. Curr. Biol. 11, R713–R724.

Zeng, L., Fagotto, F., Zhang, T., Hsu, W., Vasicek, T.J., Perry, W.L., III, Lee, J.J., Tilghman, S.M., Gumbiner, B.M., Costantini, F., 1997. The mouse *Fused* locus encodes axin, an inhibitor of the Wnt signaling pathway that regulates embryonic axis formation. Cell 90, 181–192.